Supplementary Information for

Supply of phosphate to early Earth by photogeochemistry after meteoritic weathering

Dougal J. Ritson, Stephen J. Mojzsis and John D. Sutherland

Table of contents

General experimental

Reagents and solvents were bought from Sigma-Aldrich, Alfa Aesar and Santa Cruz Biotechnology and were used without further purification. Photochemical reactions were carried out using a Rayonet RPR-200 photochemical reactor chamber, with cooling fans switched on and fitted with low pressure RPR-2537A Hg lamps purchased from Rayonet (principle emission 254 nm). Hellman QS Spectrosil 10.0 mm quartz cuvettes were used with 4 UV transparent windows. UV-Vis Spectra were acquired using a Varian 6000i UV-Vis-NIR spectrophotometer and Cary winUV software (Agilent Technologies). A Mettler Toledo SevenMulti pH/mv module fitted with a Thermo Scientific Orion 8103BN pH probe was used to measure pH, and deoxygenation of solvents was achieved by sparging with Ar for 20-30 min before use. ^{1}H And ^{31}P NMR spectra were acquired using a Bruker Ultrashield^{TM} 400 Plus (at 400.1 and 162.0 MHz, respectively) or Bruker Ascend^{TM} 400 (at 400.2 and 162.0 MHz, respectively) using HOD suppression to collect ^{1}H NMR data (reactions were run in 10% D_2O-H_2O solutions). Chemical shifts (δ) are given in ppm.

Supplementary Discussion 1

The report[1] which identified PO_4^{3-} as a by-product in a GC-MS chromatogram of a reaction involving HPO_3^{2-} and formaldehyde (CH_2O) under UV irradiation (the desired product being hydroxymethyl phosphonic acid, Supplementary Fig. 1) warranted a re-investigation for two reasons: firstly, the authors noted that the UV light source (a low pressure Hg lamp) had "a significant component at 185 nm", and the observed reactions were suggested to be dependent on radiation of this wavelength to allow photolysis of H_2O. As Earth's atmosphere should have been rich in H_2O and CO_2, light of wavelength < 200 nm would have been filtered out,[2] and if the reaction was reliant upon the radiation of 185 nm wavelength it could not be considered prebiotically plausible. Secondly, the authors reported that in the absence of other reactants, the irradiation of HPO_3^{2-} under the same conditions gave hypophosphate ($P_2O_6^{4-}$) but not PO_4^{3-}.[3] A mechanism whereby CH_2O could allow the production of PO_4^{3-} from HPO_3^{2-} under photolysis conditions was (to us) not obvious, and so we wished to confirm that in the absence of CH_2O, $P_2O_6^{4-}$ was indeed the product.

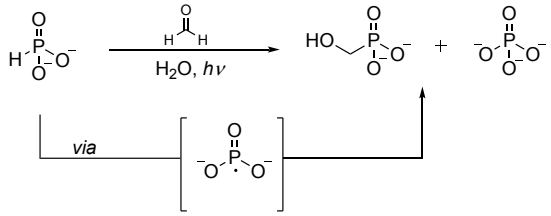

Supplementary Fig. 1 Synthesis of hydroxymethyl phosphonate and phosphate.[1]

To this end, we irradiated HPO_3^{2-} (30 mM) in degassed H_2O at pH 6.5 with a low pressure Hg lamp. By ^{31}P NMR spectroscopy we observed slow formation of a new product, the signal of which (at 0.90 ppm) integrated for ~ 38% of all phosphorus signals after 16 h irradiation. When spiked with an authentic sample of orthophosphate (PO_4^{3-}) the integration increased to ~ 56% (Supplementary Fig. 3). Whilst it could have been possible for the signals of PO_4^{3-} and $P_2O_6^{4-}$ to be coincidental, altering the pH of the sample to 2.1 or 13.0 did not reveal any other signals (the NMR signals of phosphorus oxy acids are sensitive to changes in pH and usually fluctuate to differing degrees). Furthermore, it was reported that the ^{31}P NMR shift of $P_2O_6^{4-}$ to be 14.4 ppm at pH 13.0,[4] yet no resonance at this frequency was observed in our NMR spectrum when altered to pH 13.0 (Supplementary Fig. 3, spectrum E). Repetition of the reaction using a concentration of 1 mM HPO_3^{2-} and at pH 8.0 (matching the original conditions[3] that gave their fastest rate of oxidation (see Reference 3, Fig. 1)) was then performed. After 1

h and 3 h reaction, HPO_3^{2-} and PO_4^{3-} could be seen by ^{31}P NMR spectroscopy but a signal at 14.4 ppm corresponding to $P_2O_6^{4-}$ was absent (Supplementary Fig. 4).[4] It was stated that "The reaction is quite efficient, more than 10% Na_2HPO_3 being converted to $Na_4P_2O_6$ in a few hours",[3] yet after 3 h reaction using our equipment ~ 90% of HPO_3^{2-} had been converted to PO_4^{3-} with no detection of $Na_4P_2O_6$ (Supplementary Fig. 4) and after 7 h reaction conversion of HPO_3^{2-} to PO_4^{3-} was quantitative, which indicates the UV flux of our equipment is higher than that used in the original study.[3]

A UV spectrum of HPO_3^{2-} has been reported previously in which no absorbance could be seen, but the spectral width only ranged from 220 to 290 nm.[5] We therefore decided to run our own UV analysis of HPO_3^{2-} and found that at a concentration of 1 mM at pH 6.5, HPO_3^{2-} begins to absorb UV light just below 200 nm (although $\lambda_{(max)}$ could not be determined using our equipment, it must occur at 186 nm or below, see Supplementary Figs. 5 and 6). When we irradiated EtOH (30 mM) in H_2O at pH ~ 7.5 for 4 h, signals for acetaldehyde (and the hydrate thereof) and acetate could be seen in the ^1H NMR spectrum (~ 3% in total, Supplementary Fig. 7), which is strongly suggestive that hydroxyl radicals are being generated in this system. From the data at hand it seems probable that Schwartz *et al.*[3] made an erroneous assignment and that PO_4^{3-} not $P_2O_6^{4-}$ is the product of photolysis of HPO_3^{2-} in water. If $P_2O_6^{4-}$ does form under our reaction conditions it is formed in negligible concentrations that cannot be detected by routine ^{31}P NMR spectroscopy. This then, would account for PO_4^{3-} observed in subsequent studies by the same group, obviating the proposed mechanistic requirement of CH_2O to explain oxidation of HPO_3^{2-} to PO_4^{3-}.[1] If the UV output at 185 nm (common to low pressure mercury lamps) is responsible for the observed chemistry, it may be due to the photolysis of H_2O, HPO_3^{2-} or a combination of both which gives rise to PO_4^{3-} but cannot be determined from these studies.

Supplementary Discussion 2

Following Procedure 1, in the first ~ 1 h of irradiation we observed little oxidation of HPO_3^{2-} but abundant hydrogen evolution, which we assumed resulted from reaction of $H^\bullet$ radicals with H_2S. After 2 h irradiation oxidation of HPO_3^{2-} had begun (13% PO_4^{3-}, Supplementary Fig. 8) and after 4 h and 6 h reaction, oxidation had been rapid, giving 65% and 90% of PO_4^{3-}, respectively (Supplementary Fig. 8). The rate of reaction then slows; after 8 h irradiation there was only a further increase of 4% in PO_4^{3-} (Supplementary Fig. 8). During the preparation of this manuscript, we became aware of some solution phase studies of the photochemical behaviour of HS^-/H_2S which help explain these observations.[6] At the pH of the reaction (initial pH 6.5) there is a substantial quantity of HS^- and H_2S (1st pK_a of H_2S ~ 7.1), and a significant amount of HPO_3^{2-} will exist as its monoanion (2nd pK_a of H_3PO_3 ~ 6.2[7]). Thus, after photodetachment of an electron from HS^-,[8] we had expected H_2S and $H_2PO_3^-$ to act as general acids and protonate $e^-_{(aq)}$ (see main text and Fig. 1). However, addition of $e^-_{(aq)}$ to H_2S with subsequent homolytic fission of an H-S bond is more rapid, and is presumably the dominant reaction pathway for $e^-_{(aq)}$ until H_2S (or HS_nH) is consumed (Supplementary Fig. 2, box a).[6] Hydrogen atom abstraction from H_2S by $H^\bullet$, resulting in H_2 and $HS^\bullet$, is approximately an order of magnitude faster (k = 1 x 10^{10} L.mol^{-1}.s^{-1}) than $H^\bullet$ production from $e^-_{(aq)}$ and H_2S.[6] It may also be possible for $H^\bullet$ to abstract a hydrogen atom from HS^- (although $e^-_{(aq)}$ will not react with hydrosulfide[9]) or polysulfides, HS_nH, or recombine with $H^\bullet$ (depending upon concentration) to generate more H_2. At neutral pH, $HS^\bullet$ dissociates to $H^+ + {}^-S^\bullet$ although radical dimerisation of $HS^\bullet$ is also possible (Supplementary Fig. 2, box a). $HS^\bullet$ May have a pK_a as low as 3, potentially allowing specific acid catalysed protonation of $e^-_{(aq)}$ leading to more $H^\bullet$ and thereby H_2.[6] Lastly, ${}^-S^\bullet$ radicals add to HS^- very quickly producing $HSS^{\bullet 2-}$ radical anions, with the reverse reaction being approximately 3 orders of magnitude slower. Thus, in this first phase of chemistry, H_2 production would be expected to be very rapid and, indeed, was observed. The fact that the majority of the HPO_3^{2-} remains presumably reflects the relative strength of the P-H bond of HPO_3^{2-} *vs.* S-H bonds. Furthermore, hydrogen atom abstraction by $HSS^{\bullet 2-}$ would be expected to be difficult, and it may be the slow reversal to $HS^- + {}^-S^\bullet$ which allows $H^\bullet$ abstraction from HPO_3^{2-} by ${}^-S^\bullet$. By analogy, Das *et al.* found ${}^-S^\bullet$ oxidised ferrocyanide ($Fe(CN)_6^{4-}$ efficiently but the dimer, $HSS^{\bullet 2-}$, was over an order of magnitude less efficient.[6] Photochemical oxidation of $HSS^{\bullet 2-}$ would be expected to be very slow under the reaction conditions λ_{max} = 380 nm[6]) but photooxidation of HSS^- should proceed efficiently (λ_{max} = 258 nm[10]), which can lead to polysulfides through recombination with other $RS^\bullet$ radicals

(Supplementary Fig. 2, box b. Polysulfide formation *via* two electron chemistry can also be envisaged). Thus, at longer irradiation times polysulfides may homolyse but eventually S_8 would be expected to form, which is also consistent with our observations *i.e.* after 1 – 2 h irradiation the reaction had a white turbidity and some small flecks of a white precipitate, after 8 h irradiation the solution was clear and a white precipitate had deposited on the floor of the cuvette. This also confirms the observation of Das *et al.* that polysulfides form at $[HS^-/H_2S] >$ 500 μM under UV irradiation.[6] As the reaction progresses and more sulfur is removed from solution by precipitation, the rate of reaction with HPO_3^{2-} would be expected to decrease, again consistent with our findings (*vide supra* and Supplementary Fig. 8). Although the nature of the oxidant(s) cannot be determined, it appears highly unlikely to be $H^{\bullet}$. Further evidence that the oxidant, or that the source of the oxidant, is polysulfidic in nature, was obtained as follows. A solution of NaSH was irradiated for 45 min in the absence of HPO_3^{2-}, which, if our mechanistic assumptions were correct, would allow production of polysulfide species. Introduction of HPO_3^{2-} at this point with subsequent irradiation should then allow immediate oxidation of HPO_3^{2-} to PO_4^{3-} with no lag period. Indeed this was the case, as is shown in Supplementary Fig. 11 (*vide infra*). Furthermore, when phosphite and NaSH were irradiated together for 45 min, only a trace of PO_4^{3-} was formed (Supplementary Fig. 11).

Once the phosphite radical is formed oxidation can occur *via* three mechanisms: a) recombination with a thiyl radical, b) single electron transfer, or c) dimerisation of phosphite radicals with subsequent hydrolysis (Supplementary Fig. 2, box c). Low levels of PSO_3^{3-} were observed during this reaction (Supplementary Fig. 10), which could have resulted from Pathway a) or b). Other phosphorus species, where RS = polysulfide, were not observed, but this does not indicate they were not formed. Thiophosphate is quite stable to hydrolysis under the reaction temperature and pH because the leaving group is very poor (pK_b of $S^{2-} \sim 14.0$), but if the leaving group was a polysulfide *e.g.* HS_4^-, the leaving group is vastly superior (pK_b of HS_4^- is of the order of 3.8[11]). This, coupled with the steric penalty of a P-S_nH bond, could mean the lifetime of such a species was not observable under the experimental conditions/apparatus. Although PSO_3^{3-} could result from Pathway c), by attack of HS^- on hypophosphate ($P_2O_6^{4-}$), $P_2O_6^{4-}$ is quite stable to nucleophilic attack (hydrolysis of $P_2O_6^{4-}$ to PO_4^{3-} and HPO_3^{2-} requires strongly acidic conditions (*e.g.* > 0.5 M HCl and heating[12]) and was never observed under our reaction conditions. Thus, Pathways a) and b) appear more likely.

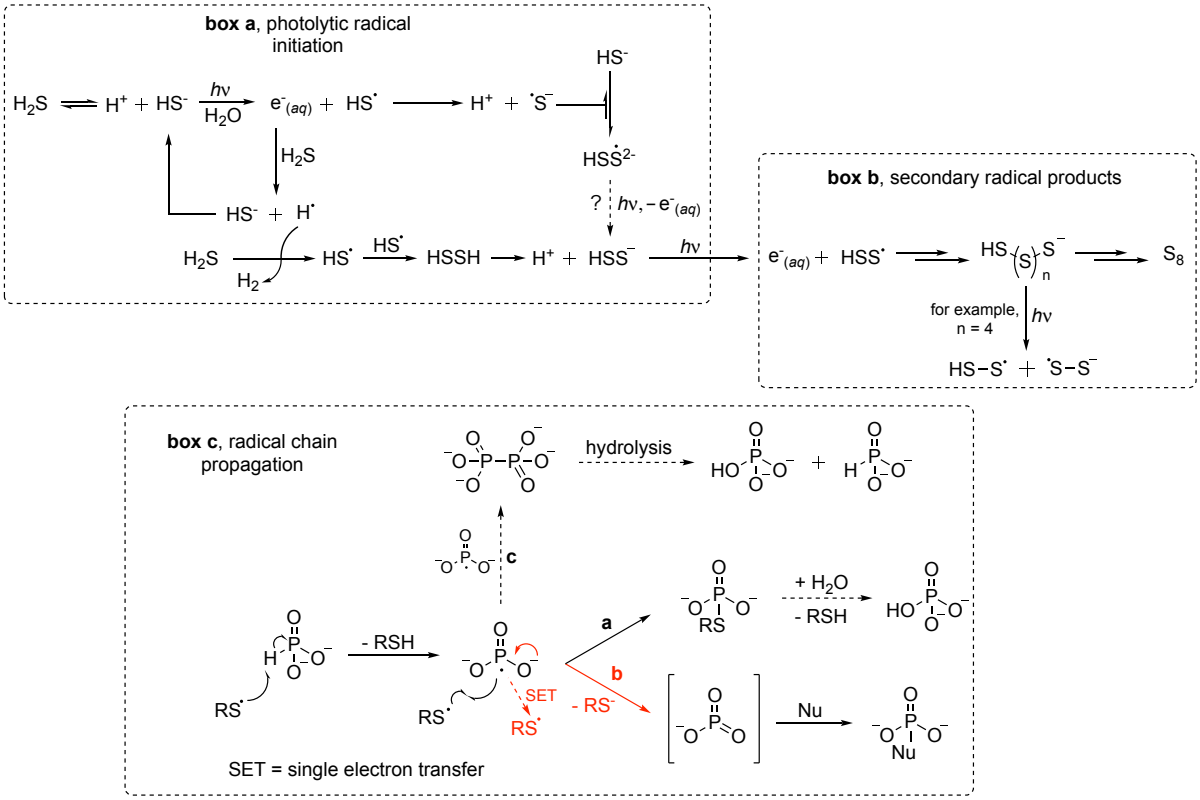

Supplementary Fig. 2 Possible mechanisms for the solution phase oxidation of HPO_3^{2-} by irradiation of HS^- (please note, the reactions depicted do not represent all possible reaction pathways, and although not drawn as such (for clarity), many of the reactions are reversible).

Supplementary Discussion 3

The calculations regarding the delivery of reduced phosphorus to Earth are based on recent models from Mojzsis *et al.*[13] From these studies, it was shown that the majority of material that accreted to Earth after 4.48 Ga is expected to have been of enstatite composition, and therefore highly reduced.[13] Two baseline models were examined wherein the total mass that was delivered to Earth during late accretion (excluding Moneta) was either 0.13 wt.% or 0.065 wt.% of Earth's present day mass and only included impactors ≥ 1 km in diameter (the 0.13 wt.% model is preferred as it comports with the lunar cratering record[14]).

Schreibersite [$(Fe,Ni)_3P$] is found in almost all enstatite chondrites. Cohenite [$(Fe,NiCo)_3C$], is also found in a few enstatite chondrites. Both carbon and phosphorus are much less abundant in enstatite chondrites than is sulfur. Sulfur is approximately ten times more abundant than carbon and it is approximately twenty-five times more abundant than is phosphorus. Consequently, only a few carbides and phosphides have been reported.

In addition to schreibersite, nickelphosphide [$(Ni,Fe)_3P$], a Ni-rich polymorph discovered in an iron meteorite, has been reported in Indarch (EH4). Even more interesting, however, is the mineral perryite [$(Ni,Fe)_5(Si,P)_2$], a mixed silicide-phosphide trigonal mineral first discovered in the peculiar Horse Creek, Colorado, USA iron. It is reported from 12EL and 4 EH enstatite chondrites. It is even reported in the small South Oman meteorite which appears to be lacking in schreibersite. Apparently, the silicon competes with phosphorus when the oxygen fugacity is so low. One curiosity illustrating the utterly reduced mineralogical environments of enstatite chondrites is the absence of any reported phosphate minerals. In Iron meteorites schreibersite is common, but a number of phosphates have also been reported. No phosphates, however, are reported for enstatite chondrites. As small phosphate mineral grains are occasionally reported in the literature as 'phosphate' when a mineralogical assay is not available, it would not be surprising if a more thorough search of the references and/or the literature might turn up a report of small phosphates. One might expect occasional phosphates to be present in some primitive unequilibrated EH3 or EL3 chondrite as in small inclusions. Any such phosphates, however, would apparently be very minor constituents.

Cohenite is found, but rarely. The conditions that allow cohenite to coexist with both iron and graphite are somewhat problematic. Both Mason and Buchwald report that cohenite is commonly associated with graphite in some iron meteorites (*e.g.* IAB irons),[15] sometimes present in others, and apparently absent in still others. As a general rule, however, the enstatite chondrites were formed in even more reducing conditions than many or even most irons, so

what general principles are involved are not clear.

Supplementary Note 1

Calculation for reduced phosphorus content of Moneta:

Mass of Moneta is estimated to be ~ 1×10^{23} kg.
The average reduced phosphorus content of enstatite chondrites (EH and EL) is ~ 1690 ppm.[16]
Therefore we could expect 0.169% of Moneta's mass to be reduced phosphorus, which is
$0.169 \times (1 \times 10^{23}) = 1.69 \times 10^{20}$ kg

Calculation for the mass of reduced phosphorus delivered by late accretion (not including Moneta) *i.e.* from 4.50 Ga to 3.50 Ga, using the 0.13 wt% model:

Total mass accreted mass from 4.50 Ga to 3.50 Ga = 7.8×10^{21} kg.
Assuming all accreted materials were of enstatic composition *i.e.* containing 1690 ppm reduced phosphorus,[16] we could expect the total of reduced phosphorus delivered to Earth during late accretion to be
0.169% of 7.8×10^{21} kg = 1.32×10^{19} kg

Calculation for reduced phosphorus content of an enstatite meteorite 1 km in diameter:

Density of enstatite chondrites is ~ 3.6 g/cc.[17]
1 km object (assumed spherical) has a volume ~ 0.52 km^3, mass = 1.872×10^{12} kg
The average reduced phosphorus content of enstatite chondrites (EH and EL) is ~ 1690 ppm.[16]
Therefore we could expect a 1 km object to contain
0.169% of $1.872 \times 10^{12} = 3.164 \times 10^{9}$ kg of reduced phosphorus

Experimental details, UV and NMR spectra

Supplementary Procedure 1: UV Photolysis of phosphite

Sodium phosphite pentahydrate (0.060 mmol, 13 mg) was dissolved in degassed 10% D_2O (1 mL) and the pH adjusted to 6.5 with degassed HCl. The volume was made up to 2 mL with degassed 10% D_2O, then the solution was transferred to a quartz cuvette and irradiated for the desired amount of time, after which it was analysed by ^{31}P NMR spectroscopy.

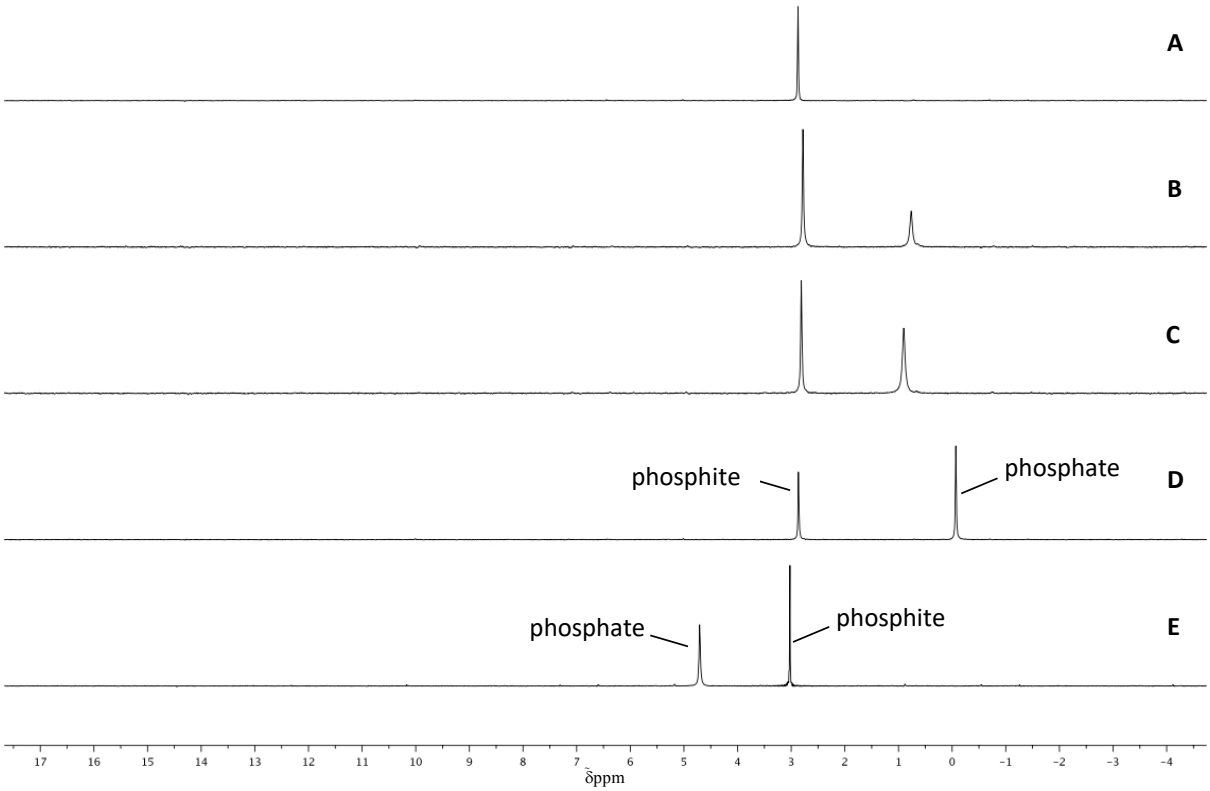

Supplementary Fig. 3 Photochemical oxidation of phosphite to phosphate in H_2O. A – ^{31}P NMR Spectrum of a commercial sample of phosphite at pH 6.5; B – ^{31}P NMR Spectrum of the reaction mixture according to Supplementary Procedure 1 after 16 h and pH re-adjusted to 6.5; C – As spectrum B, spiked with NaH_2PO_4 and re-adjusted to pH 6.5; D – As spectrum C, pH adjusted to 2.1; E – As spectrum D, pH adjusted to 13.0.

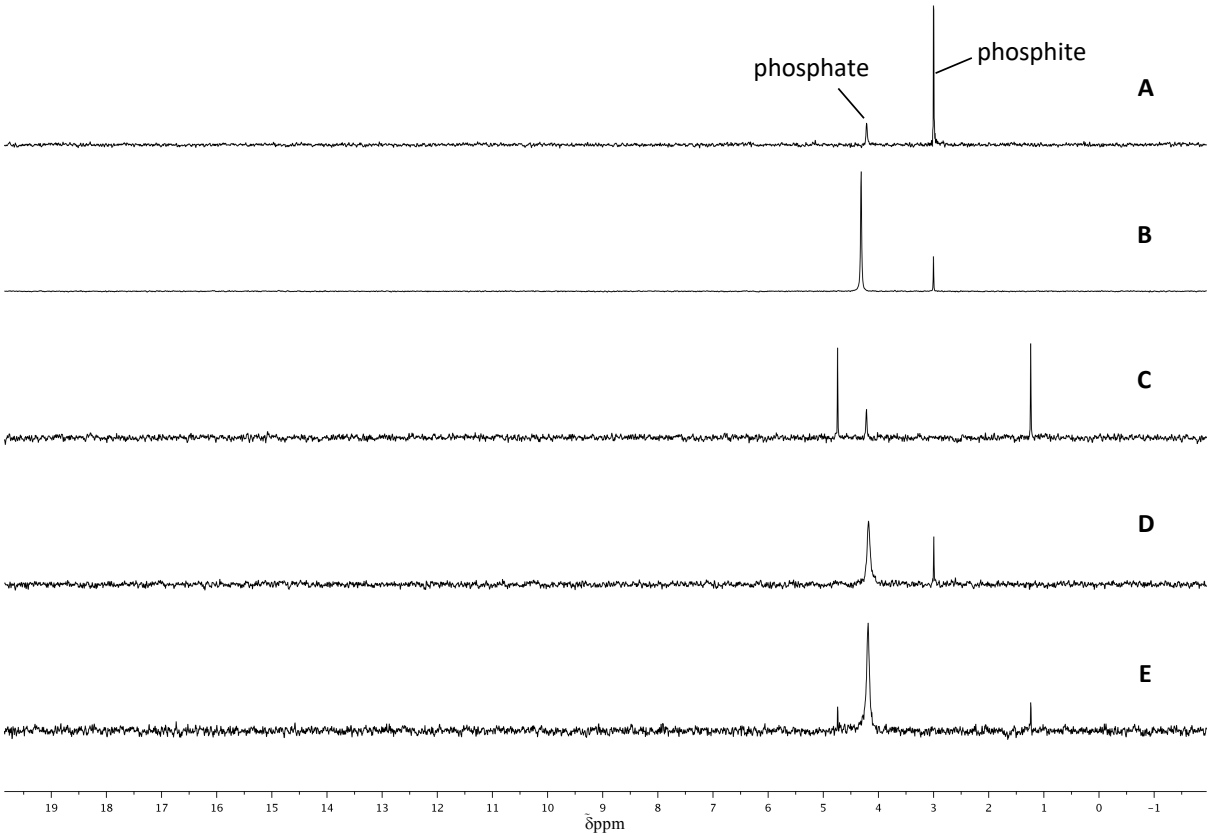

Supplementary Fig. 4 Photochemical oxidation of phosphite to phosphate under conditions reported by Schwartz *et al.*[3] A – ^{31}P NMR Spectrum of the reaction mixture after 1 h of irradiation of a 1 mM solution of phosphite at pH 8.0 in degassed 10% D_2O (pH of solution adjusted to 13.0 before acquiring the NMR spectrum); B – As spectrum A spiked with an authentic sample of PO_4^{3-}; C – As spectrum A but with coupling to ^{1}H nuclei; D – ^{31}P NMR Spectrum of the reaction mixture after 3 h of irradiation of a 1 mM solution of phosphite at pH 8.0 in degassed 10% D_2O (pH of solution adjusted to 13 before acquiring the NMR spectrum); E – As spectrum D but with coupling to ^{1}H nuclei.

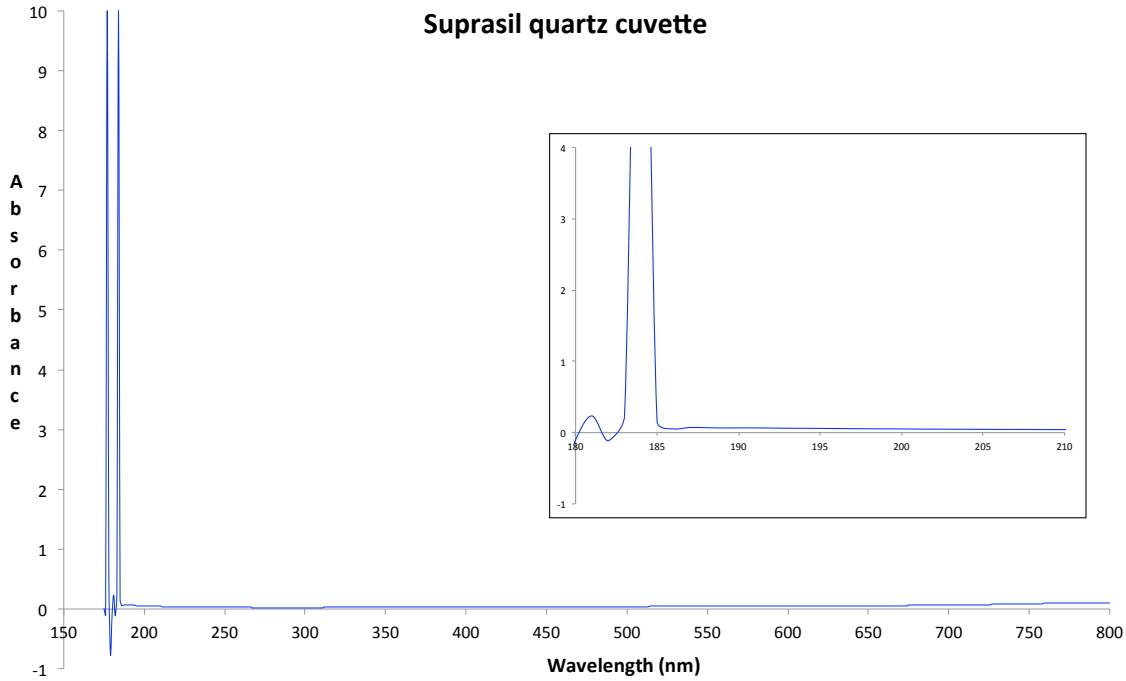

Supplementary Fig. 5 UV-Vis Spectrum of a typical Spectrosil quartz cuvette used in our photochemical reactions (no liquid phase was included). At 185 nm transmission of light is starting to be interrupted, but how much of this was due to air (O_2, CO_2 and H_2O) and how much due to quartz beginning to absorb UV light could not be determined (from the manufacturers website,[18] the quartz used was transparent to >60% of the light at 185 nm).

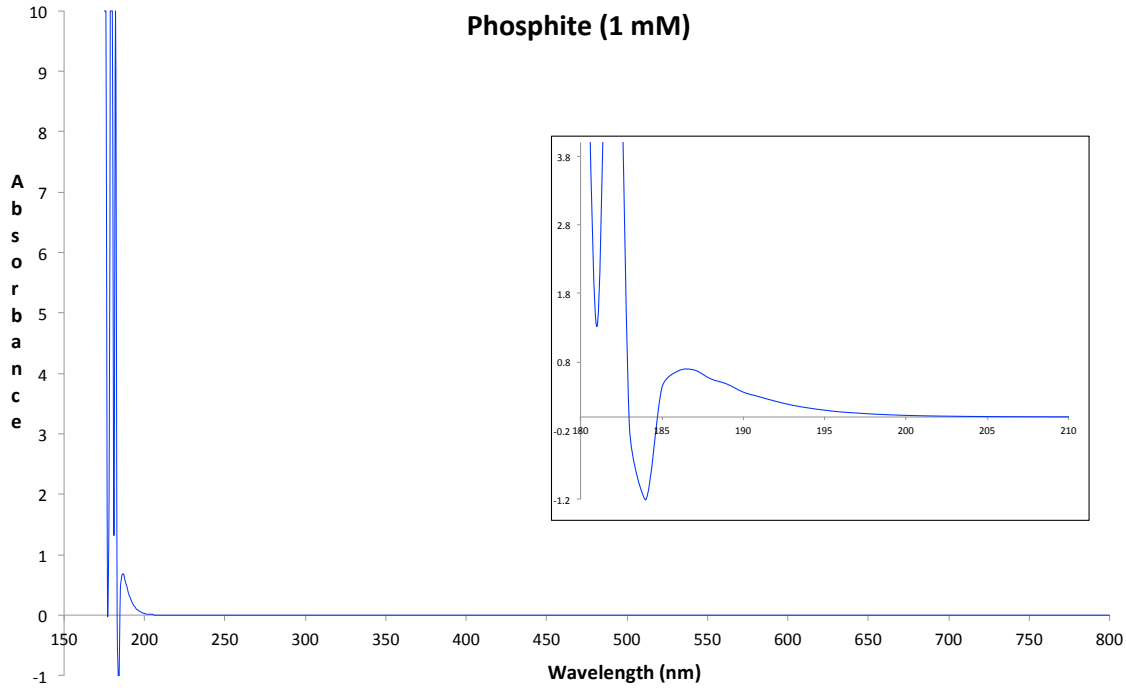

Supplementary Fig. 6 UV-Vis Spectrum of a 1 mM solution of disodium phosphite pentahydrate at pH 6.5 in deionised water (a control spectrum of deionised water has already been subtracted from the original spectrum containing PO_3^{2-}, resulting in the spectrum above).

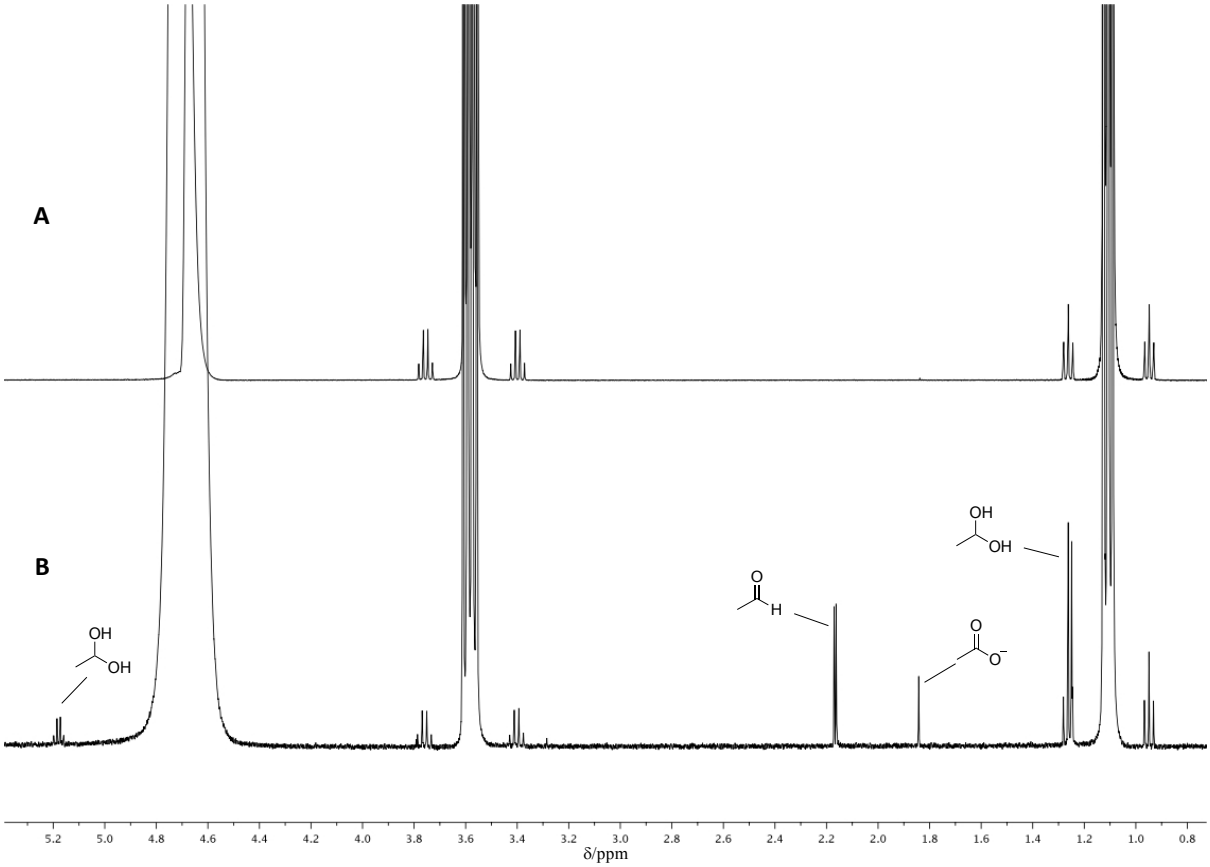

Supplementary Fig. 7 Photochemical oxidation of EtOH in H_2O by photolysis. A – ^1H NMR Spectrum of a commercial sample of EtOH; B – ^1H NMR Spectrum of the irradiation products of EtOH (30 mM) in degassed 10% D_2O at pH 7.5 after 4 h.

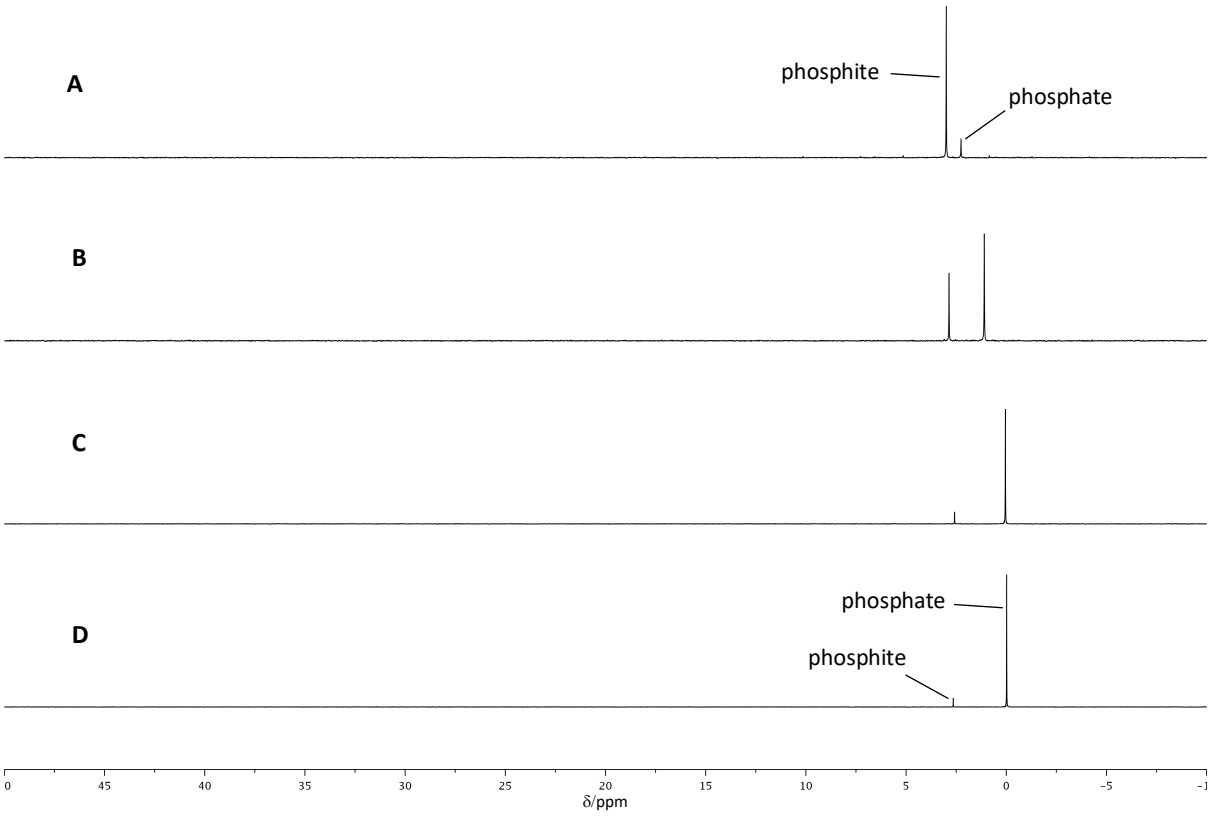

Supplementary Fig. 8 Photochemical oxidation of phosphite to phosphate in the presence of HS^-. A – ^{31}P NMR Spectrum of the irradiation of phosphite after 2 h according to Procedure 1 (yield of phosphate ~ 13%); B – ^{31}P NMR Spectrum of the irradiation of phosphite after 4 h according to Procedure 1 (yield of phosphate ~ 65%); C – ^{31}P NMR Spectrum of the irradiation of phosphite after 6 h according to Procedure 1 (yield of phosphate ~ 90%); D – ^{31}P NMR Spectrum of the irradiation of phosphite after 8 h according to Procedure 1 (yield of phosphate ~ 94%, small differences in chemical shifts due to differences in pH).

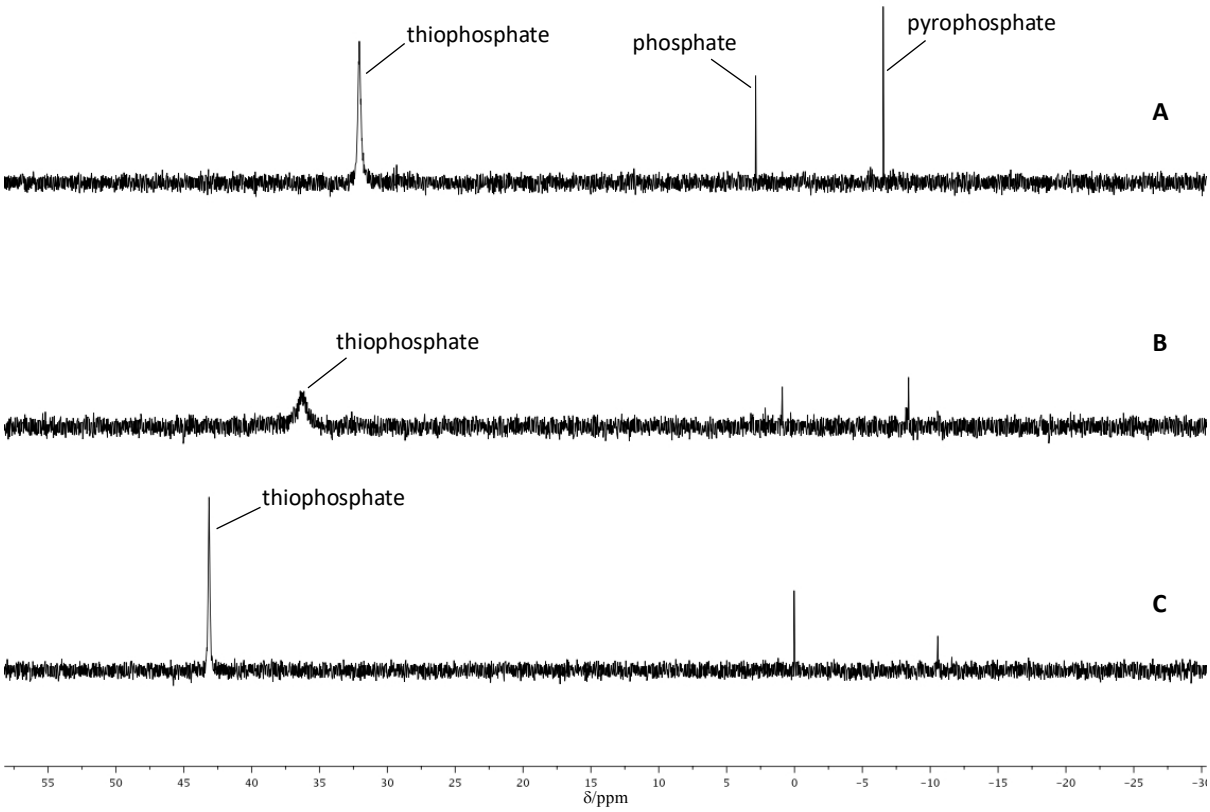

Supplementary Fig. 9 Effect of pH on the thiophosphate ^{31}P NMR signal. A – ^{31}P NMR Spectrum of a commercial sample of thiophosphate at pH 11.5 (this commercial sample included impurities of phosphate 3% and pyrophosphate 3%); B – ^{31}P NMR Spectrum of a commercial sample of thiophosphate at pH 6.5; C – ^{31}P NMR Spectrum of a commercial sample of thiophosphate at pH 4.7.

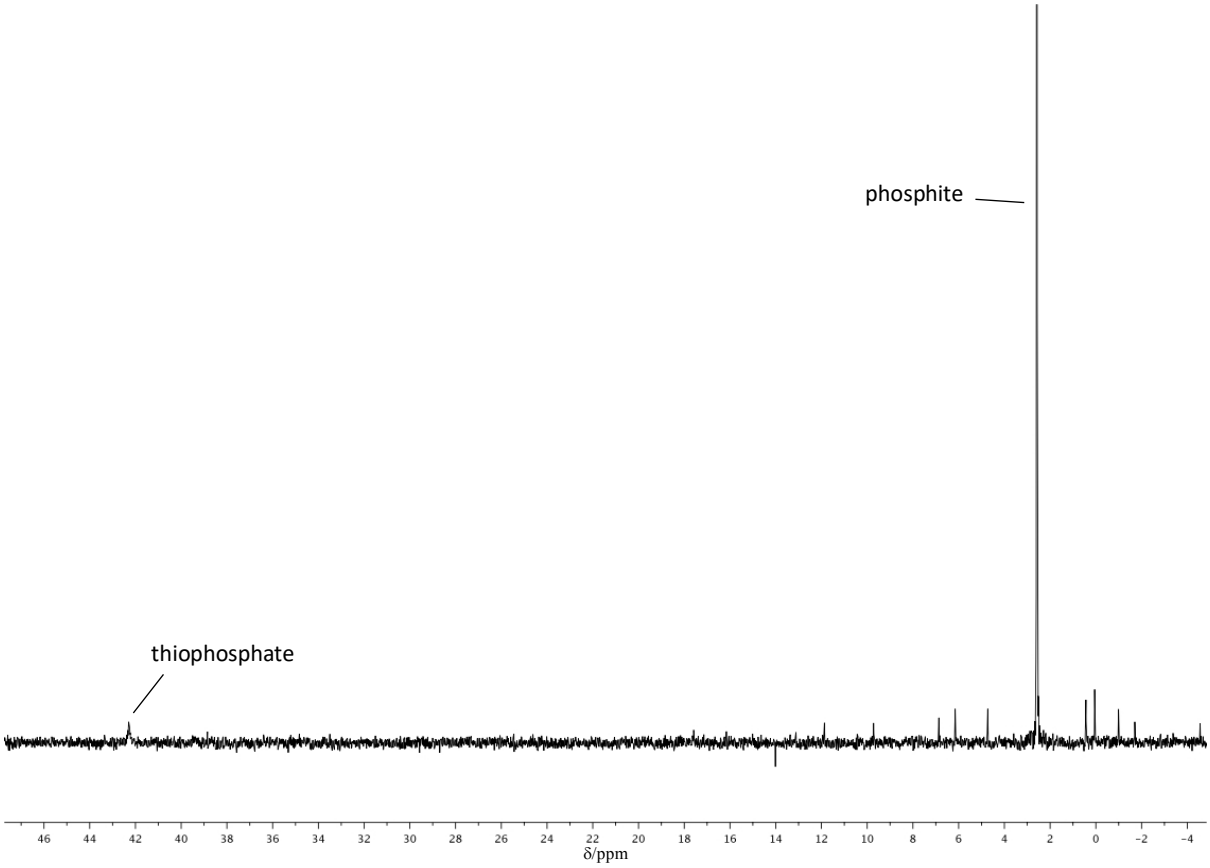

Supplementary Fig. 10 Photochemical oxidation of phosphite to thiophosphate using HS^-. ^{31}P NMR Spectrum of the irradiation of phosphite after 1.5 h according to Procedure 1 (the sample was acidified with 1 M HCl before NMR spectroscopy).

Supplementary Procedure 2: Indication of polysulfide involvement in the mechanism of oxidation of phosphite

a) NaSH (>60%, 0.100 mmol, 9 mg) was dissolved in degassed 10% D_2O (1 mL) in an Eppendorf and the pH was adjusted to 6.5 with degassed HCl, then the volume was made up to 1.9 mL with degassed 10% D_2O. The reaction was irradiated for 45 min after which time the solution was yellow with some white turbitity. $Na_2PO_3.5H_2O$ (0.060 mmol, 13 mg) Was added and the pH re-adjusted to 6.7, then the reaction was irradiated for a further 1 h at which point a ^{31}P NMR spectrum was acquired (Supplementary Fig. 11, spectrum A).

b) Sodium phosphite pentahydrate (0.060 mmol, 13 mg) and $NaSH.xH_2O$ (>60%, 0.100 mmol, 9 mg) were dissolved in degassed 10% D_2O (1 mL) in an Eppendorf and the pH was adjusted to 6.5 with degassed HCl. The volume was made up to 2 mL, then the solution was transferred to a quartz cuvette and irradiated for 45 min after which time a ^{31}P NMR spectrum was acquired (Supplementary Fig. 11, spectrum C).

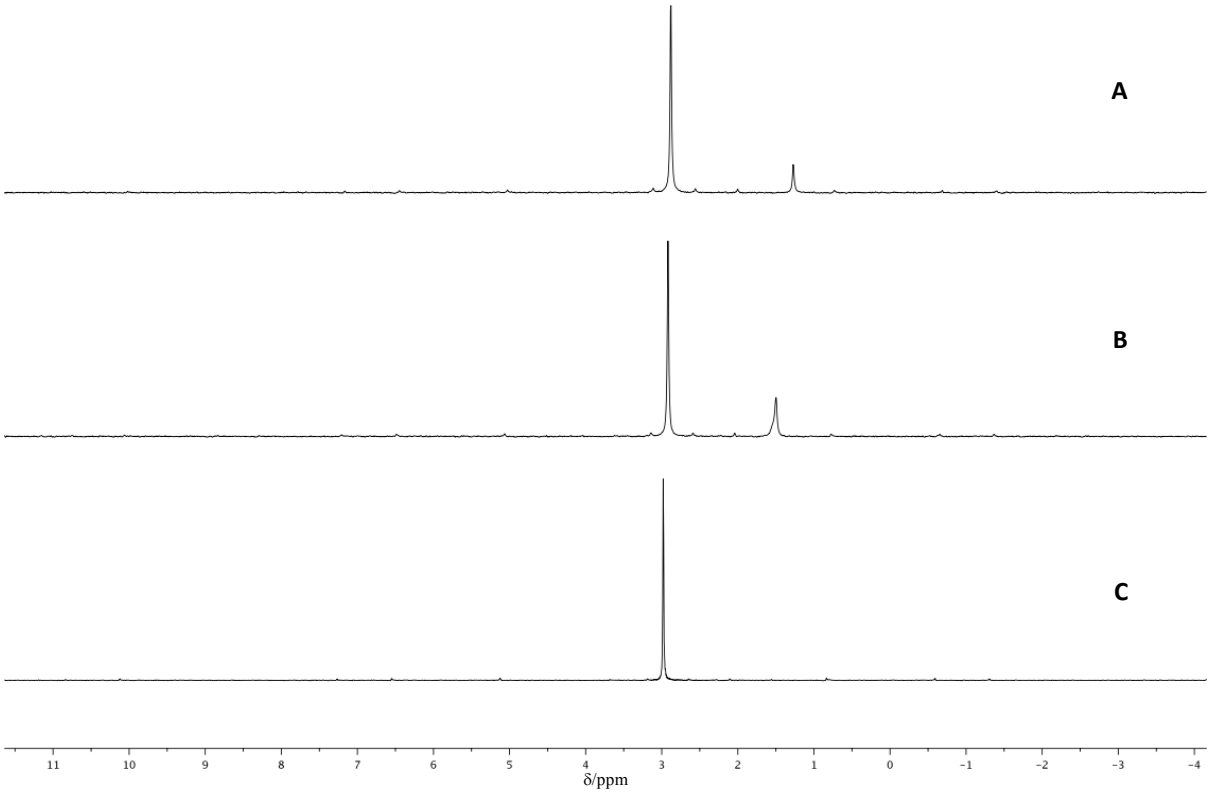

Supplementary Fig. 11 Photochemical oxidation of phosphite by the products of photolysis of an aqueous solution of NaSH (see supplementary Discussion 2). A – ^{31}P NMR Spectrum of the reaction according to Supplementary Procedure 2, a) after 1 h of irradiation of the phosphite and polysulfide solution, yield of phosphate ~ 14%; B – As spectrum A spiked with an authentic sample of phosphate; C – ^{31}P NMR Spectrum of the reaction according to Supplementary Procedure 2, b) after 45 min of irradiation (< 1% phosphate had been formed).

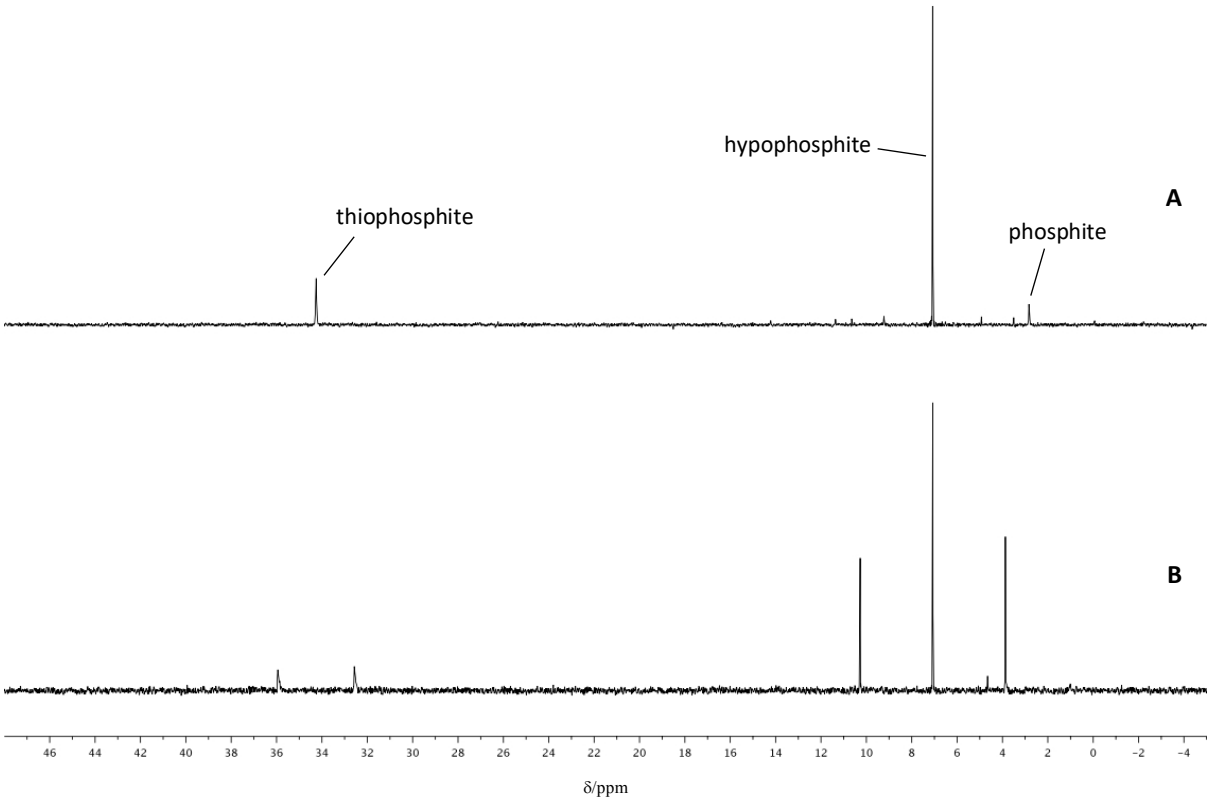

Supplementary Fig. 12 Photochemical reaction of hypophosphite in the presence of HS^-. A – ^{31}P NMR Spectrum of the irradiation of hypophosphite after 20 min according to Procedure 2; B – As spectrum A but with coupling to ^1H nuclei. The downfield shift of phosphoryl P-S species appears to be a general trend, for example see Ref. 19.

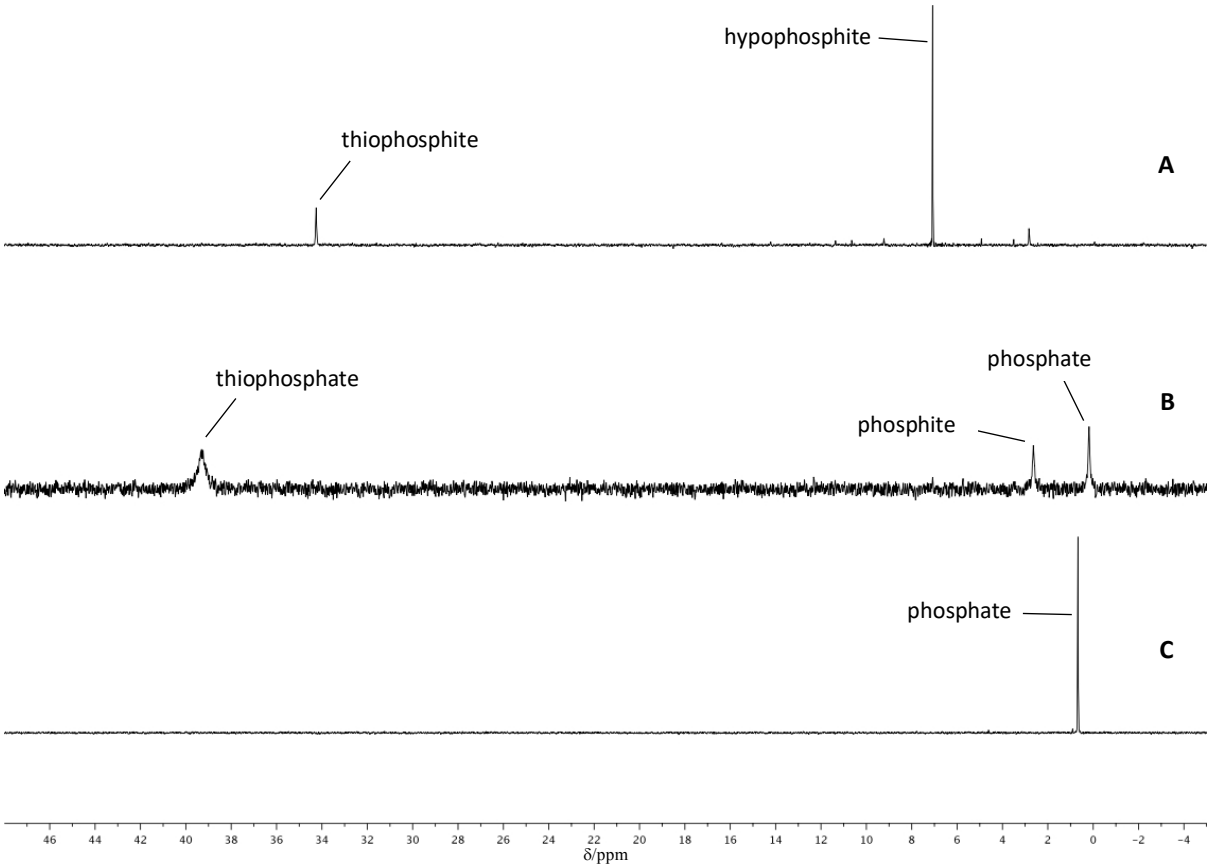

Supplementary Fig. 13 Photochemical reaction of hypophosphite in the presence of HS^-. A – ^{31}P NMR Spectrum of the irradiation of hypophosphite after 20 min according to Procedure 2; B – as spectrum A after 1 h irradiation; C – as spectrum A after 5.5 h irradiation.

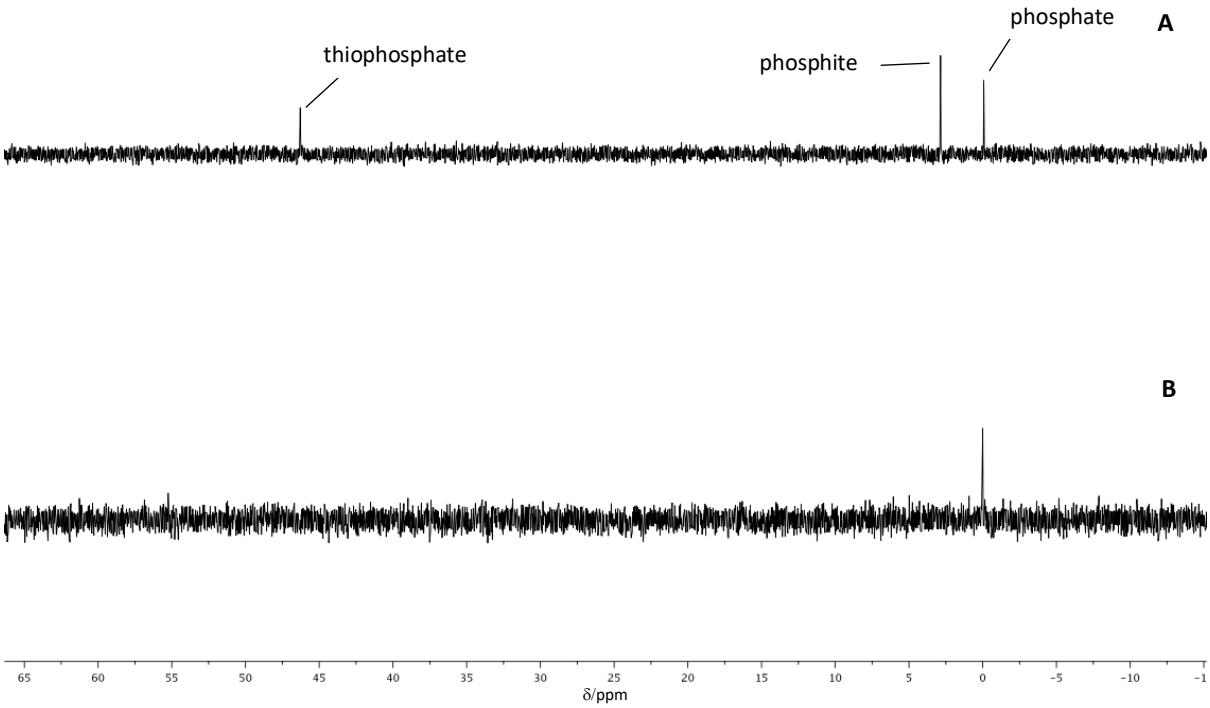

Supplementary Fig. 14 Photochemical reaction of hypophosphite in the presence HS^- at low concentration. A – ^{31}P NMR Spectrum of the irradiation of hypophosphite after 10 min according to Procedure 3 (sample acidified with HCl before spectroscopy to improve resolution of the thiophosphate signal – see Supplementary Fig. 9); B – ^{31}P NMR Spectrum of the irradiation of hypophosphite after 4 h according to Procedure 3 (sample acidified with HCl before spectroscopy to improve resolution of the thiophosphate signal – see Supplementary Fig. 9).

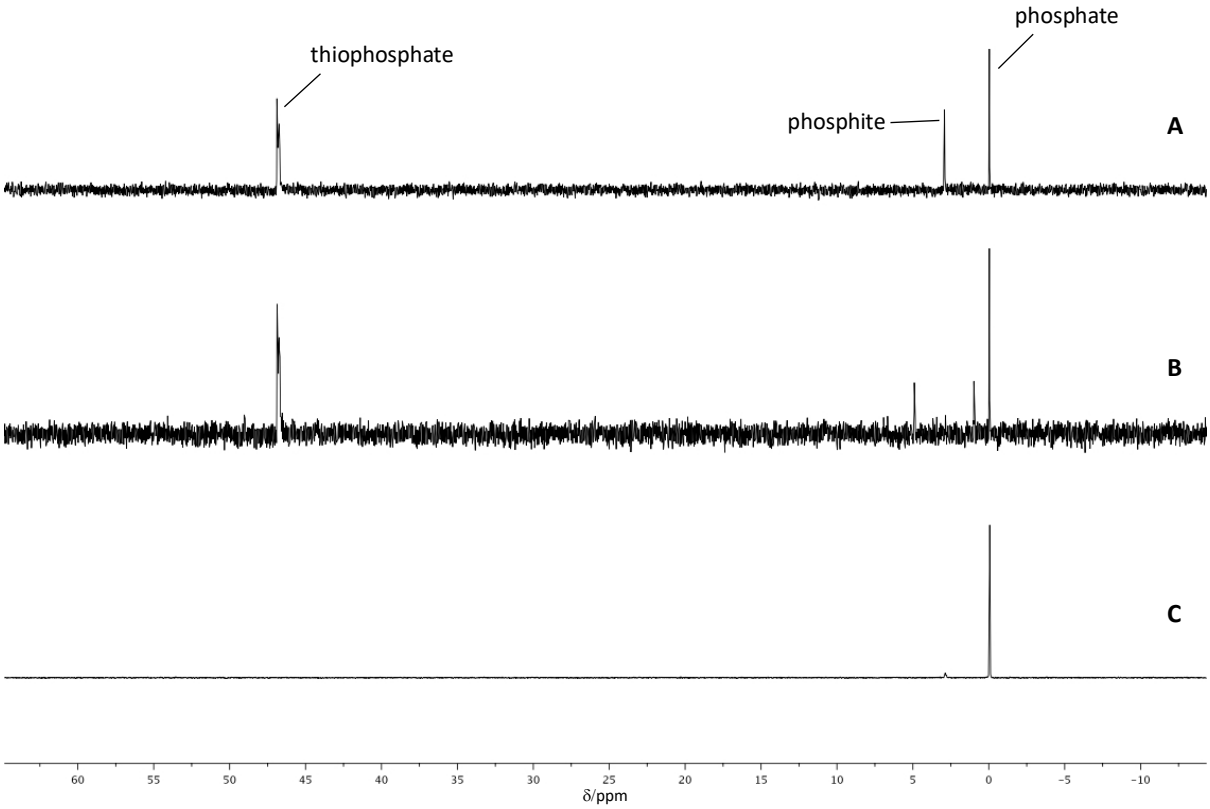

Supplementary Fig. 15 Photochemical reaction of hypophosphite in the presence of HS^- at pH 9.0. A – ^{31}P NMR Spectrum of the reaction after irradiation of hypophosphite for 2 h according to Procedure 4 (sample acidified with HCl before spectroscopy to improve resolution of the thiophosphate signal – see Supplementary Fig. 9); B – As spectrum A, but with coupling to ^{1}H nuclei; C – ^{31}P NMR Spectrum of the reaction after irradiation of hypophosphite for 8 h according to Procedure 4 (sample acidified with HCl before spectroscopy to improve resolution of the thiophosphate signal – see Supplementary Fig. 9).

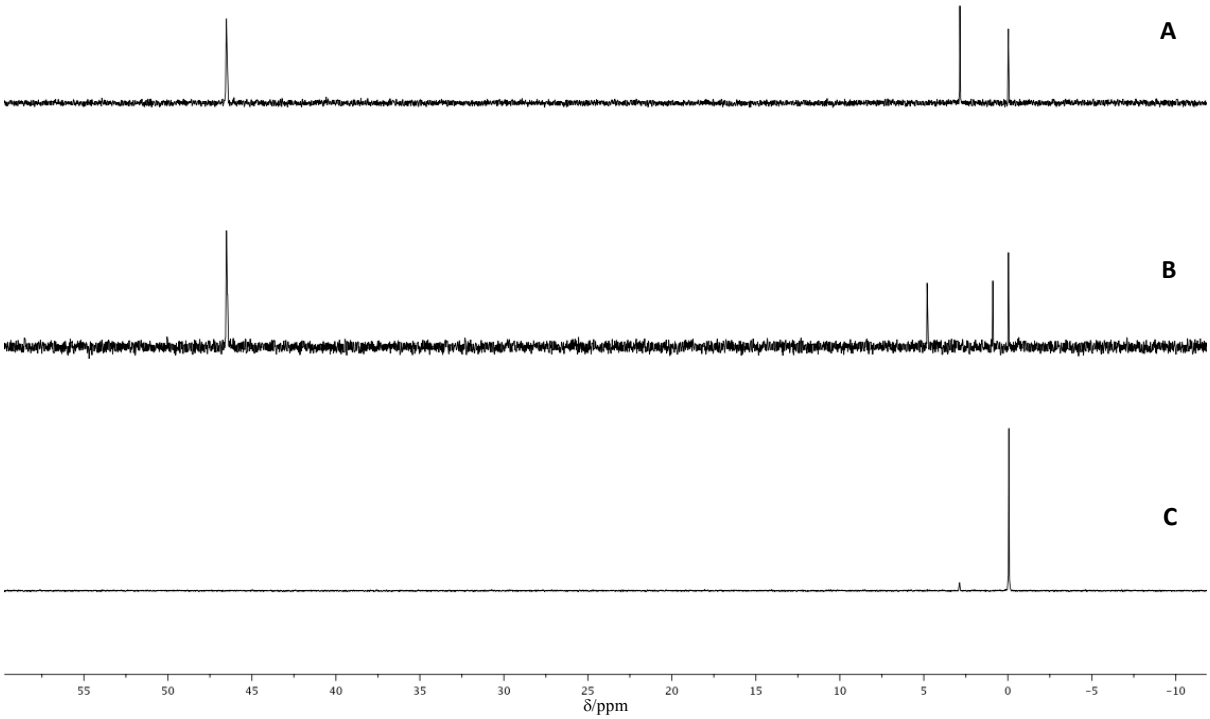

Supplementary Fig. 16 Photochemical reaction of hypophosphite in the presence of HS^- at pH 10.3. A – ^{31}P NMR Spectrum of the reaction after irradiation of hypophosphite for 20 min according to Procedure 4 but with an initial pH of 10.3 (sample acidified with HCl before spectroscopy to improve resolution of the thiophosphate signal – see Supplementary Fig. 9); B – As spectrum A, but with coupling to ^1H nuclei; C – ^{31}P NMR Spectrum of the reaction after irradiation of hypophosphite after 8 h irradiation according to Procedure 4 but with an initial pH of 10.3 (sample acidified with HCl before spectroscopy to improve resolution of the thiophosphate signal – see Supplementary Fig. 9).

Supplementary Procedure 3: Attempted synthesis of DAP

Hypophosphorus acid (50% wt., 0.060 mmol, 6.2 μL), NH_4OH (25%, 50 μL) and NaSH (9 mg, 0.100 mmol) were dissolved in degassed 10% D_2O (1 mL) and pH was adjusted to 7.0 or 9.2 with degassed 5 M HCl. The volume was made up to 2 mL with degassed 10% D_2O and the solution was transferred to a quartz cuvette and irradiated for the desired amount of time, after which it was analysed by ^{31}P NMR spectroscopy.

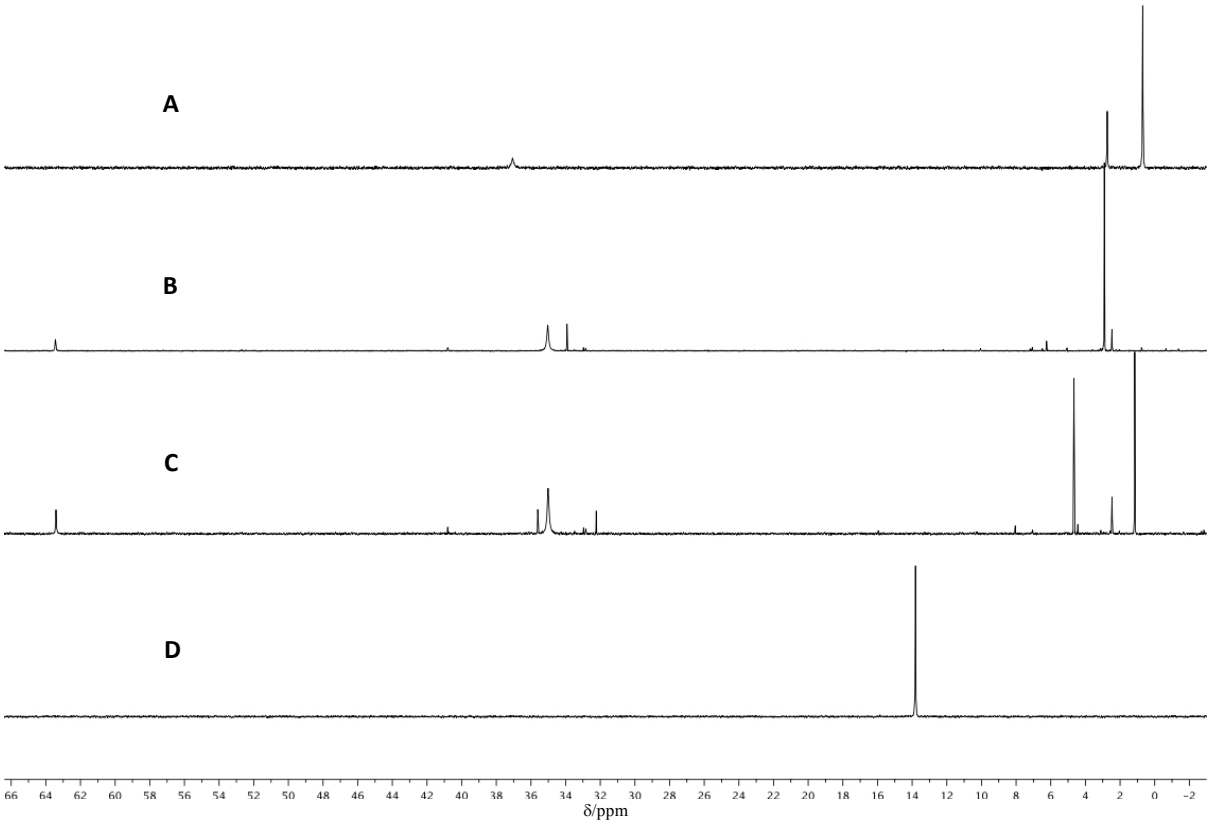

Supplementary Fig. 17 Attempted synthesis of DAP *via* photochemical oxidation of hypophosphite. A – ^{31}P NMR Spectrum of the reaction after irradiation of hypophosphite for 1.5 h according to Supplementary Procedure 3, initial pH 7.0; B – ^{31}P NMR Spectrum of the reaction after irradiation of hypophosphite for 1.5 h according to Supplementary Procedure 3, initial pH 9.2; C – As spectrum B but with coupling to ^{1}H nuclei. Note the new signal in spectrum B at δ 64.8 is not split and we therefore tentatively assign it to $H_2NPSO_2^{2-}$; D – ^{31}P NMR Spectrum of a sample of DAP, prepared according to Ref. 20.

Supplementary Procedure 4: Attempted synthesis of DAP

a) Hypophosphorus acid (50% wt., 0.060 mmol, 6.2 μL), NH_4OH (25%, 50 μL) and NaSH (9 mg, 0.100 mmol) were dissolved in degassed 10% D_2O (1 mL) and the pH was adjusted to 9.2 with degassed 5 M HCl. The volume was made up to 2 mL with degassed 10% D_2O and the solution was transferred to a quartz cuvette and irradiated for 1.5 h, after which it was analysed by ^{31}P NMR spectroscopy.

b) A sample (500 μL) was taken at the end of the reaction (Supplementary Procedure 4, a)) and 25% NH_4OH (200 μL) was added. The sample was sealed and kept for 2 d at room temperature after which a ^{31}P NMR spectrum was acquired (Supplementary Fig. 18, C).

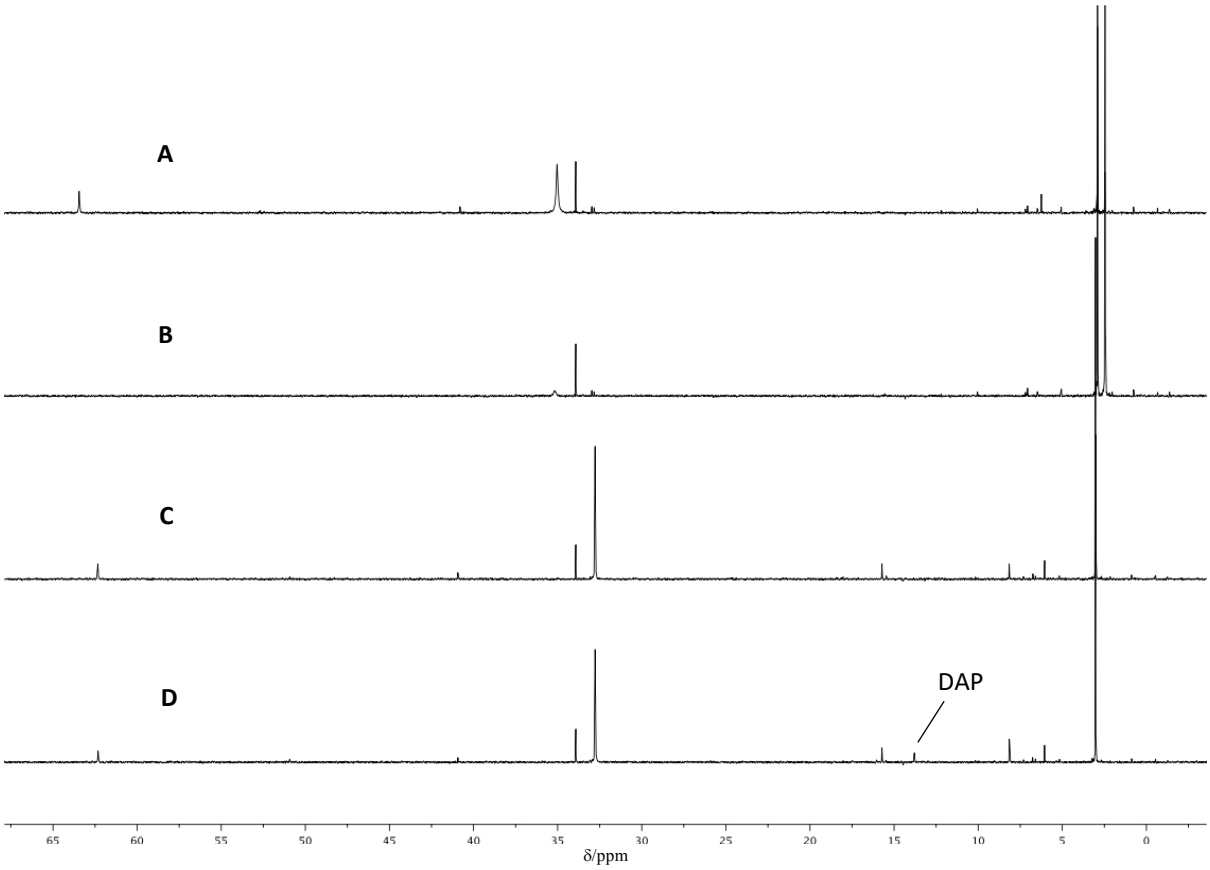

Supplementary Fig. 18 Attempted synthesis of DAP by nucleophilic displacement of S^{2-} from the presumed intermediate $H_2NPSO_2^{2-}$ (see Supplementary Fig. 17). A – ^{31}P NMR Spectrum of the reaction after irradiation of hypophosphite for 1.5 h according to Supplementary Procedure 4, a); B – As spectrum A after being heated to 70 °C for 3 h; C – ^{31}P NMR Spectrum of the reaction after 2 d according to Supplementary Procedure 4, b); D – As spectrum C, after spiking with an authentic sample of DAP (prepared as in Ref. 20).

References

1. de Graaf, R. M., Visscher, J. & Schwartz, A. W. A plausibly prebiotic synthesis of phosphonic acids. *Nature,* **378** 474-477 (1995).
2. Ranjan, S. & Sasselov, D. D. Influence of the UV environment on the synthesis of prebiotic molecules. *Astrobiol.* **16**, 68-88 (2016).
3. Schwartz, A. W. & van der Veen, M. Synthesis of hypophosphate by ultraviolet irradiation of phosphite solutions. *Inorg. Nucl. Chem. Lett.* **9**, 39-41 (1973).
4. Pasek, M. A. & Lauretta, D. S. Aqueous corrosion of phosphide minerals from iron meteorites: a highly reactive source of prebiotic phosphorus on the surface of the early Earth. *Astrobiol.* **5**, 515-535 (2005).
5. Buck, R. P., Singhadeja, S. & Rogers, L. B. Ultraviolet absorption spectra of some inorganic ions in aqueous solutions. *Anal. Chem.* **26**, 1240-1242 (1954).
6. Das, T. N., Huie, R. E., Neta, P. & Padmaja, S. Reduction potential of the sulfhydryl radical: pulse radiolysis and laser flash photolysis studies of the formation and reactions of •SH and HSSH•$^-$ in aqueous solutions. *J. Phys. Chem. A* **103**, 5221-5226 (1999).
7. Eykyn, T. R. & Kuchel, P. W. Scalar couplings as pH probes in compartmentalized biological systems: ^{31}P NMR of phosphite. *Magn. Reson. Med.* **50**, 693-696 (2003).
8. Sauer, M. C., Crowell, R. A. & Shkrob, I. A. Electron photodetachment from aqueous anions. 1. Quantum yields for generation of hydrated electron by 193 and 248 nm laser photoexcitation of miscellaneous inorganic anions. *J. Phys. Chem. A* **108**, 5490-5502 (2004).
9. Karmann, W., Meissner, G. & Henglein, A. Pulsradiolyse des schwefelwasserstoffs in wäßriger lösung. *Z. Naturforsch. B* **22**, 273-282 (1967).
10. Franzfehër, F. & Münzner, H. Beiträge zur chemie des schwefels, 62. Ultraviolett-absorptionsspektren kettenförmiger schwefelverbindungen. *Chem. Ber.* **96**, 1131-1149 (1963).
11. Steudel, R. *Inorganic Polysulfanes H_2S_n with n > 1. Elemental Sulfur and Sulfur-rich Compounds II. Topics in Current Chemistry, Vol. 231* (Springer, Berlin, Heidelberg, 99-126, 2003). Ed: Steudel, R.
12. Yoza, N., Koga, I. & Ohashi, S. Kinetic study on the hydrolysis of hypophosphate. *J. Inorg. Nucl. Chem.* **33**, 1435-1442 (1971).

13. Mojzsis, S. J., Brasser, R., Kelly, N. M., Abramov, O. & Werner, S. C. Onset of giant planet migration before 4480 million years ago. *Astrophys. J.* **881**, doi: doi.org/10.3847/1538-4357/ab2c03 (2019).
14. Werner, S. C. Moon, Mars, Mercury: basin formation ages and implications for the maximum surface age and the migration of gaseous planets. *Earth Planet. Sci. Lett.* **400**, 54-65 (2014).
15. See (and references therein): Keil, K. Enstatite meteorites and their parent bodies. *Meteoritics* **24**, 195-208 (1989).
16. Lodders, K. & Fegley, B. *The Planetary Scientist's Companion* (Oxford. University Press, Oxford, 1998).
17. Macke, R. J., Consolmagno, G. J., Britt, D. T. & Hutson, M. L. Enstatite chondrite density, magnetic susceptibility, and porosity. *Meteorit. Planet. Sci.* **45**, 1513-1526 (2010).
18. http://www.hellma-analytics.com/text/129/en/pg_id,40/cuvettes.html.
19. Jaffe, E. K. & Cohn, M. ^{31}P Nuclear magnetic resonance spectra of the thiophosphate analogues of adenine nucleotides; effects of pH and Mg^{2+} binding. *Biochem.* **17**, 652-657 (1978).
20. Gibard, C., Bhowmik, S., Karki, M., Kim, E-K. & Krishnamurthy, R. Phosphorylation, oligomerization and self-assembly in water under potential prebiotic conditions. *Nat. Chem.* **10**, 212-217 (2018).